Review Article
cnj.araku.ac.ir

☑ Cite This: Colloid Nanosci. J. 3(4) (2025) 742-752 DOI: 10.66224.3.4.742

# Silica Sulfuric Acid-Modified $ZrFe_2O_4$ Magnetic Nanoparticles as an Eco-Friendly Catalyst for the One-Pot Three-Component Synthesis of Tetrahydrobenzo[b]pyran

***Maryam Borzooei, Masoomeh Norouzi****

*Department of Chemistry, Faculty of Science, Ilam University, Ilam, Iran*

**ARTICLE INFO**

***Article History:***
*Received 2025-12-19*
*Revised 2026-01-29*
*Accepted 2026-02-02*
*Published 2025-12-01*

***Corresponding Authors:***
*Maryam Borzooei*
*Email:*
*maryamborzooei78@gmail.com*

**ABSTRACT**

Magnetic nanoparticle-based supported catalysts are a promising class of stable and recyclable materials for green organic reactions. In this study, a novel sulfonic acid-functionalized zirconium ferrite nanostructure ($ZrFe_2O_4$@$SiO_2$–$SO_3H$) was successfully synthesized and characterized by fourier transform infrared (FT-IR), scanning electron microscopy (SEM), transmission electron microscopy (TEM) image, X-ray atomic mapping spectrum, spectroscopy, energy-dispersive X-ray (EDX) analysis, brunauer, emmett, teller (BET)/Langmuir plot and vibrating-sample magnetometry (VSM) analyses, confirming its well-designed core-shell structure. This magnetic nanocatalyst exhibits a high density of Brønsted acid sites along with easy magnetic separation, providing an efficient and reusable substrate for organic reactions. Its catalytic activity was investigated in the synthesis of tetrahydrobenzo[b] pyran derivatives, where the reactions proceeded in a short time with good to excellent yields (up to 98%) under mild conditions. Furthermore, the catalyst maintained its high performance over five consecutive cycles without significant loss of efficiency, indicating its remarkable chemical stability and magnetic recyclability. These results demonstrate the strong potential of $ZrFe_2O_4$@$SiO_2$–$SO_3H$ as a robust and environmentally friendly nanocatalyst for high-yield organic syntheses and emphasize the importance of sulfonic acid-functionalized systems in the design of recyclable catalytic platforms.

**KEYWORDS:** *Zirconium Ferrite nanoparticles; catalyst; sulfonic acid; Tetrahydrobenzo[b]pyran*

## 1. Introduction

Currently, in the 21st century, nanotechnology, as one of the most important revolutionary events in the science and technology industry, focuses on the use of nanoscale compounds. The unique size and physical properties of these compounds have brought them countless advantages that have become the most fundamental research fields in modern science. Magnetic nanoparticles (MNPs), especially spinel ferrites, are used as the basis of catalysts due to their favorable biocompatibility, non-toxicity and chemical stability. The magnetic recovery capability of MNPs is their most important advantage. This capability allows for easy separation of MNPs from the reaction medium without using traditional methods (centrifugation and filtration), using only an external magnet, which is much more effective than previous methods, which is also a great advantage for the development of more efficient and environmentally friendly chemical processes [1-11]. These nanoparticles significantly enhance the activity of catalysts in applications such as organic synthesis, environmental remediation, and drug production by facilitating the binding between the catalyst and the reactants. The ability of MNPs to respond to magnetic fields enables rapid and efficient separation, simple recovery, and thus reduced waste and recycling costs [12-23].

Despite advantages, magnetic cores face challenges such as aggregation, corrosion, and limited selectivity. Surface modification is employed to improve stability and efficiency. The presence of surface hydroxyl groups on MNPs facilitates functionalization with various

modifiers. Coating MNPs with silica ($SiO_2$) is a common and advantageous strategy: it activates surface groups, forms stable M–O–Si bonds, and enhances performance. Silica coatings help prevent aggregation by reducing interparticle interactions and shielding dipole–dipole forces [24-33].

Besides, Sulfuric acid ($H_2SO_4$) is a strong Brønsted acid widely used in organic and multicomponent reactions but is highly corrosive and requires careful handling. $SO_3H$ active solids imitate concentrated $H_2SO_4$ and offer safer, cheaper, and easier-to-handle alternatives for catalysis, electrocatalysis, and water treatment [3]. Combining sulfuric acid strength with the spinel ferrite support enables durable, efficient, and magnetically recoverable heterogeneous catalysts for a variety of organic transformations.

In the current research, $ZrFe_2O_4@SiO_2–SO_3H$ catalyst with a core-shell structure has been designed. This magnetic nanocatalyst, utilizing sulfonic acid, provides abundant acidic active sites for organic reactions. The remarkable features of this compound are the retention of catalytic efficiency after multiple reuses and high structural stability. Ultimately, this system enables reactions to be carried out with high yields in a short time and is an important step in the development of sustainable industrial processes.

## 2. Experimental Section

### 2.1. Synthesis of $ZrFe_2O_4$ nanoparticles

The synthesis of $ZrFe_2O_4$ nanoparticles was carried out in a 250mL a double neck round bottom flask under a nitrogen atmosphere to prevent oxidation. Initially, 100 mL of deionized water was heated to 80°C; then, 10 mmol of $ZrOCl_2.8H_2O$ salt was added to it and the solution was magnetically stirred until it became clear. In the next step, 20 mmol of $FeCl_2.4H_2O$ was added to the solution. The co-precipitation process was initiated by gradually adding solid sodium hydroxide (NaOH) pellets to the solution and it was observed that with increasing pH, its color changed to black, indicating the formation of magnetic zirconium ferrite nanoparticles ($ZrFe_2O_4$). After the formation of a black suspension, high-speed magnetic stirring was continued for another 30 minutes to complete the reaction process. Finally, after the solution cooled to ambient temperature, the nanoparticles were separated using an external magnet and washed several times with deionized water to remove excess ions and impurities. The resulting black solid was finally placed in an oven at 80°C for 12 hours.

### 2.2. Preparation of $ZrFe_2O_4@SiO_2$

The surface modification process was performed to improve the surface properties of magnetic zirconium ferrite nanoparticles. In this method, 2 g of synthesized $ZrFe_2O_4$ magnetic nanoparticles was added to 100 mL of ethanol. This mixture was placed in an ultrasonic bath for one hour to disperse the particles well in the solvent and break possible agglomerates. Then, 40 ml of heated deionized water, 20 ml of ammonia solution and 10.72 g of polyethylene glycol (PEG-400) were added to the reaction mixture. Finally, 4 ml of tetraethyl orthosilicate (TEOS) was added to the mixture and stirred for 48 hours at room temperature. During this time, the TEOS hydrolysis reaction and the formation of a silica layer on the surface of the nanoparticles took place. After the reaction was completed, the obtained product was washed with deionized water and ethanol. The product was dried in an oven at 80 °C.

### 2.3. Synthesis of $ZrFe_2O_4@SiO_2–SO_3H$

In the final step of the synthesis of the target catalyst, 1 g of $ZrFe_2O_4@SiO_2$ was dispersed in n-hexane solvent in an ultrasonic bath for 30 minutes. Then, the reaction mixture was placed in an ice bath and 1.5 mL of chlorosulfonic acid was slowly added dropwise over 30 minutes and stirred for 4 hours at room temperature to complete the reaction. Next, the final product $ZrFe_2O_4@SiO_2–SO_3H$ was washed with n-hexane and at each step, the nanoparticles were separated using a strong external magnet. Finally, the resulting magnetic nanocatalyst was dried at 80°C for 12 hours. This catalyst was used to synthesize Tetrahydrobenzo[b] pyran compounds (All steps of catalyst synthesis are shown in Scheme 1).

### 2.4. General method for the synthesis of Tetrahydrobenzo[b]pyran

In a 10 mL flask, a mixture of dimedone (1 mmol), malononitrile (1 mmol), aldehyde (1 mmol), and 5 mg of the nanomagnetic catalyst $ZrFe_2O_4@SiO_2–SO_3H$ in ethanol solvent were stirred under reflux conditions. The progress of the reaction was periodically monitored by thin layer chromatography (TLC) with a solvent mixture of ethyl acetate/n-hexane (2:8). After the reaction was completed, the catalyst was separated

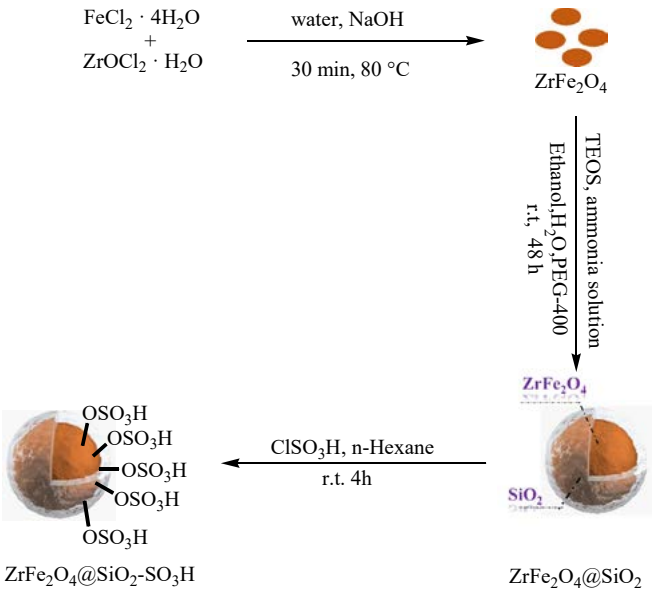


**Scheme 1.** Preparation of $ZrFe_2O_4@SiO_2–SO_3H$ magnetic nanocatalyst

using an external magnet. The final product was purified by recrystallization from hot ethanol. The desired products have been studied by $^1H$ NMR spectroscopy.

## 3. Result and Discussion

### *3.1. Catalyst Characterization*

The FT IR spectrum analysis of the $ZrFe_2O_4@SiO_2–SO_3H$ catalyst in three consecutive steps confirms the successful synthesis of a magnetic nanocatalyst. In the spectra taken from $ZrFe_2O_4$, $ZrFe_2O_4@SiO_2$ and $ZrFe_2O_4@SiO_2–SO_3H$, there are two characteristic peaks at 3400 and 560 $cm^{-1}$, which are related to the hydroxyl group (O-H) bonds and the metal oxide (M-O) groups, respectively. The confirmation of the formation of a silicate shell around the magnetic zirconium ferrite nanoparticles was well demonstrated by the appearance of peaks related to Si–O –Si bonds in the range of 1000-1200 $cm^{-1}$ and also the region of 957 $cm^{-1}$. The presence of acidic groups in the catalyst under study can be proven by referring to the broad peak observed in the range of 3391 $cm^{-1}$, which is related to the stretching vibration of the hydroxyl groups in the $SO_3H$ structure (Figure 1).

In line with our earlier study [3], XRD patterns for both $ZrFe_2O_4$ nanoparticles and the $ZrFe_2O_4@SiO_2–SO_3H$ magnetic nanocatalyst in the 2θ range of 10–80° indicate the formation of the cubic spinel phase. Accordingly, in this crystal lattice, the distribution of $Zr^{4+}$ ions in tetrahedral and octahedral sites has led to changes in the magnetic responses of the nanoparticles due to the difference in ionic radius with iron cations and also the occurrence of structural fluctuations. By attaching sulfonic acid groups to the synthesized nanomagnetic substrate, a decrease in the intensity of diffraction peaks and an increase in background noise were observed along with broad peaks in the 22–30° region, which indicates the coating of the core with a shell of amorphous compounds. Based on quantitative analyses performed on the 35.5° index peak, the average crystallite size of the material has increased from 29.5 nm in the pure state to 44.3 nm after surface modification. These changes in the obtained diffraction pattern indicate the stability of the magnetic phase after the surface modification process and the successful immobilization of $SO_3H$ groups on zirconium ferrite nanoparticles.

The elemental composition of the magnetic nanocatalyst $ZrFe_2O_4@SiO_2–SO_3H$ was analyzed using EDX analysis as shown in Figure 2. The characteristic peaks of zirconium (Zr) and iron (Fe) in the resulting spectrum indicate the formation of the desired spinel ferrite as the magnetic core of the nanocatalyst. In addition, the formation of a silica layer around it is well confirmed by the presence of silicon (Si) and oxygen (O) peaks. It is important to observe the sharp sulfur (S) peak in this spectrum, which clearly indicates the successful functionalization of the nanoparticle surface with sulfonic acid groups.

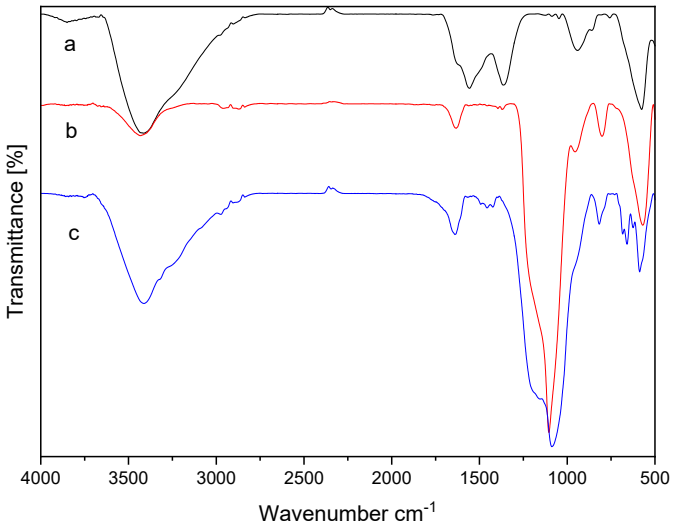


**Fig. 1.** FT-IR spectra of (a) ZrFe2O4, (b) ZrFe2O4@SiO₂, and (c) ZrFe₂O₄@SiO₂–SO₃H

Elemental Mapping analysis shown in Figure 3 was taken to investigate the distribution of elements in the magnetic nanocatalyst structure. Based on the results of this analysis, zirconium (Zr) and iron (Fe) elements as the main scaffolds are distributed in a uniform and completely similar pattern throughout the structure. In addition, the uniform distribution of silicon (Si) and oxygen (O) elements proves the successful presence of a silica shell around the magnetic core. Also, the homogeneous distribution of sulfur (S) element throughout the nanocatalyst structure indicates the functionalization of the surface with sulfonic acid ($SO_3H$) groups, which well confirms the decisive and effective role of acidic active centers in increasing the efficiency of heterogeneous catalysts.

The SEM images shown in Figure 4 confirm the successful synthesis of the $ZrFe_2O_4$@$SiO_2$–$SO_3H$ magnetic nanocatalyst. Based on the analysis of these images, the nanoparticles have spherical or quasi-spherical morphology and the average particle size is estimated to be in the range of 30–50 nm. The observation of the rough and uneven surface in the captured images can definitely confirm the formation of a core-shell structure or hybrid composite in which the $ZrFe_2O_4$ magnetic core is successfully coated by silica sulfuric acid.

The results of the transmission electron microscopy analysis shown in Figure 5 clearly reveal the distinct hierarchical structure of the $ZrFe_2O_4$@$SiO_2$–$SO_3H$ magnetic nanocatalyst. The TEM images show in more detail the unique morphology of this catalyst, which resembles the structure of an Echinops flower. The numerous nano-petals seen in this structure radiate from a central core and form large chain-like clusters, which provide a high specific surface area for the nanocatalyst and facilitate the efficient diffusion of reactants and products, leading to a significant improvement in the catalytic performance of this structure.

The surface properties and porosity of the $ZrFe_2O_4$@$SiO_2$–$SO_3H$ nanocatalyst were evaluated through nitrogen adsorption and desorption isotherms, which confirmed the mesoporous nature of the structure (Figure 6). According to BET analysis, the specific surface area of this material was determined to be 11.253 $m^2/g$ and the average pore diameter was 20.025 nm, which is a good indication of the formation of nanoscale pores on the nanocatalyst network. The data obtained in the Langmuir diagram with a specific surface area of 17.574 $m^2/g$ indicate a strong interaction between the adsorbed atmospheric molecules and the surface active sites, especially the sulfonic acid groups and the silica coating around the magnetic core of this nanocatalyst. In addition, considering the calculated total pore volume ($5.6337\times10^{-2}$ $cm^3/g$) along with the appropriate diameter of the pores, provides good access to acidic active centers, which ultimately improves the efficiency of the catalyst in chemical processes.

The magnetic properties of the $ZrFe_2O_4$@$SiO_2$–$SO_3H$ nanocomposite were evaluated using the vibrating sample magnetometer (VSM) technique. Aligning with findings from our previous study

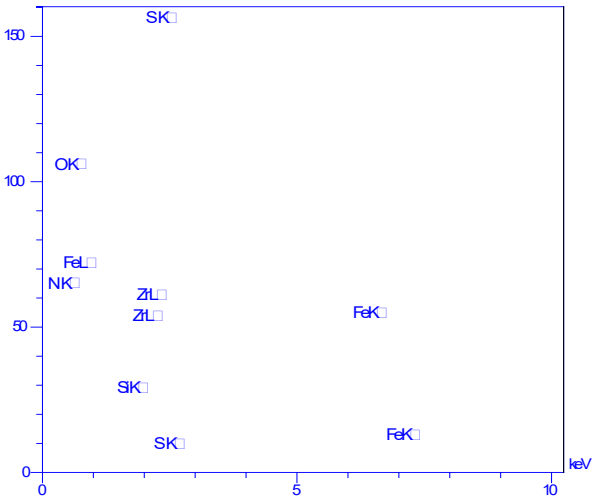


**Fig. 2.** EDX analysis of $ZrFe_2O_4$@$SiO_2$–$SO_3H$

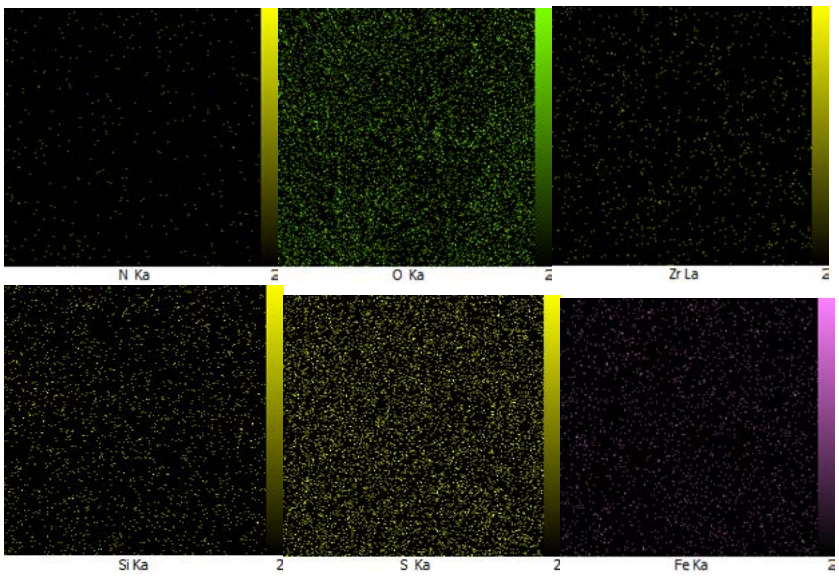


**Fig. 3.** Elemental mapping analysis of $ZrFe_2O_4$@$SiO_2$–$SO_3H$

[3], the saturation magnetization (MS) value for these nanoparticles was measured to be 5.1 emu/g, while the corresponding values for pure $ZrFe_2O_4$ and $ZrFe_2O_4$@$SiO_2$ were reported to be 18.3 emu/g and 9.49 emu/g, respectively. The decreasing trend of MS in the final sample confirms the successful deposition of the silica shell and then the surface functionalization with sulfonic acid groups, which act as non-magnetic layers to reduce the saturation magnetization of the overall structure. However, the above magnetic nanocatalyst still exhibit a favorable magnetic response, such that rapid and complete separation of the catalyst from the reaction mixture is easily possible using only an external magnet.

### *3.2. Catalytic Study*

After structural analysis of the magnetic nanocatalyst $ZrFe_2O_4$@$SiO_2$–$SO_3H$, its catalytic ability in the multicomponent reaction of one-pot synthesis of heterocyclic compounds Tetrahydrobenzo[b]pyran was investigated. For this purpose, benzaldehyde was used as a model reaction. Initially, in order to investigate the role

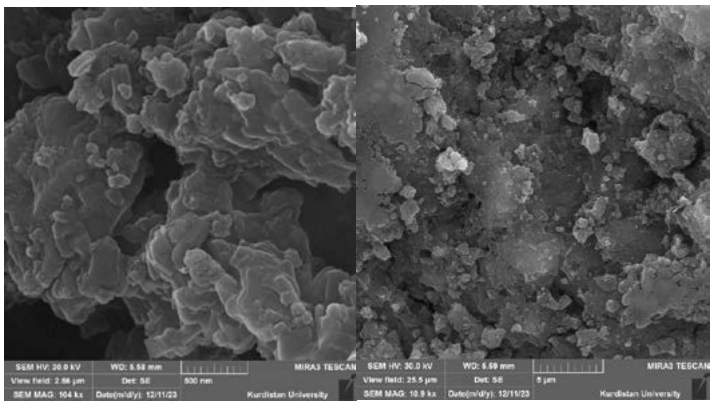

**Fig. 4.** FE-SEM images of $ZrFe_2O4@SiO_2–SO_3H$

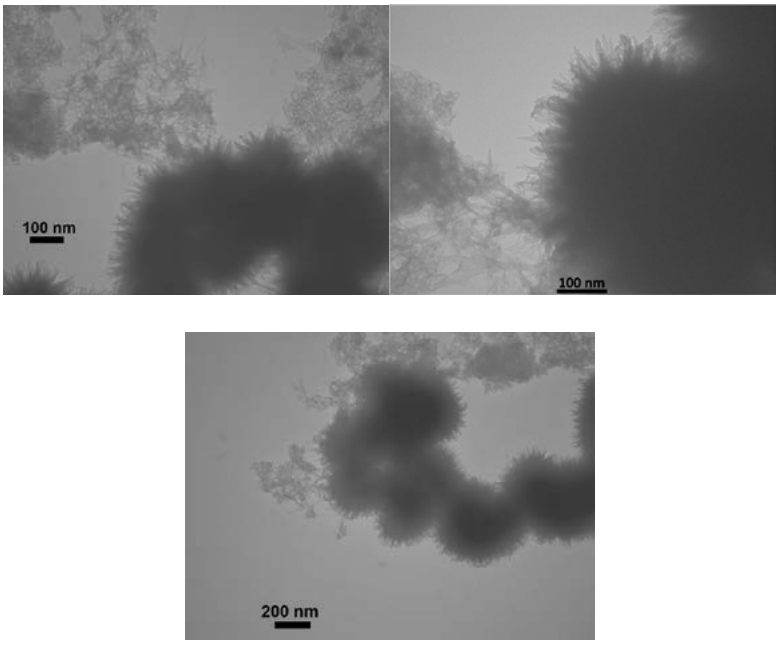


**Fig. 5.** TEM images of $ZrFe_2O_4@SiO_2–SO3H$

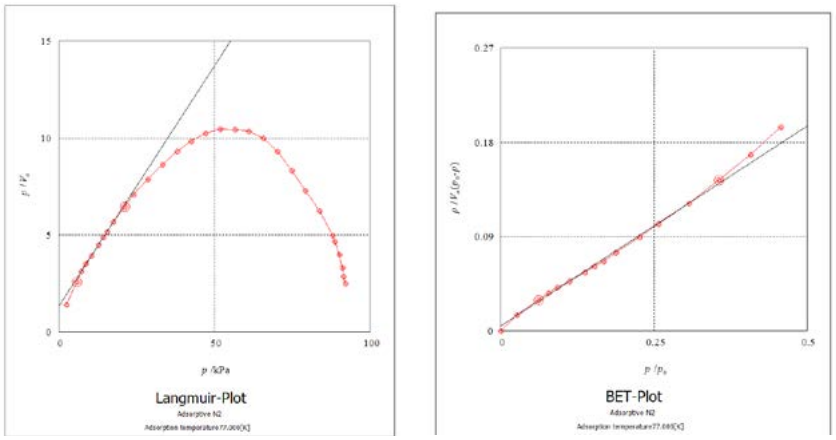


**Fig. 6.** BET and Langmuir plot for $ZrFe_2O_4@SiO_2–SO_3H$.

of the catalyst, the reaction was carried out in its absence, and no progress was observed after 120 minutes. Then, in order to optimize the reaction conditions and investigate the parameters affecting the efficiency, the effects of different amounts of catalyst, solvent type and temperature were investigated. Green solvents water, ethanol and water/ethanol mixture were evaluated as potential solvents. The results showed that using ethanol as a solvent, with a small loading of 5 mg of the synthesized magnetic nanocatalyst, leads to a yield of 97% in a short time of 25 minutes. Ethanol was chosen because it provides optimal conditions for the interaction between the reactants and the catalyst, as well as the appropriate polarity to dissolve the starting materials and product. In addition, according to the XRD results, the small crystal size of the catalyst and its uniform distribution (observed in the SEM/TEM images) lead to an increase in the surface area available for the reaction and improved catalytic performance. $SO_3H$ groups also play an important role in increasing the reaction rate by creating appropriate acidity. Finally, the effect of temperature on the reaction efficiency was also investigated. The reaction was carried out at room temperature, 100 °C and under reflux conditions. The results showed that carrying out the reaction under reflux conditions is the most appropriate choice to achieve the highest efficiency, because this temperature provides the activation energy necessary for the reaction. Overall, optimization of reaction parameters based on the results of structural analyses and experimental investigations led to achieving a high yield of 97% in the synthesis of Tetrahydrobenzo[b]pyran heterocyclic compounds (Table 1).

After obtaining the optimal reaction conditions, a wide range of different aldehydes were investigated in the synthesis of Tetrahydrobenzo[b]pyran compounds. As shown in Table 2, the aromatic aldehydes used had both electron-donating and electron-withdrawing groups. Based on the results obtained, the studied catalyst was able to proceed the reaction well in reasonable times with good to excellent yields.

The possible mechanism for the synthesis of Tetrahydrobenzo[b]pyran compounds that we envision is that initially, a Knoevenagel condensation formed between an aromatic aldehyde and malononitrile yields an α, β-unsaturated compound (intermediate I). In the next step, dimedone is converted to the enolate form (as a nucleophile) by the presence of a catalyst and attacks the β- carbon of the double bond of intermediate I, forming intermediate II through Michael addition. Finally, the final product is obtained by intramolecular Thorpe-Ziegler cycloaddition.

### 3.3. Reusability of the catalyst

One of the current concerns is the synthesis of an efficient catalytic system that can be used multiple times. Multi-stage recovery of the catalyst is very

**Table 1.** Evaluation of the reaction parameter on the synthesis of Tetrahydrobenzo[b]pyran over the catalysis of $ZrFe_2O_4@SiO_2–SO_3H$

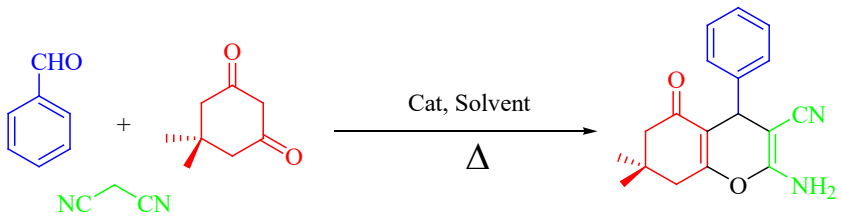


| Entry | Catalyst | Catalyst amount (mg) | Solvent | Temperature (°C) | Time (min) | Yield (%) |
|---|---|---|---|---|---|---|
| 1 | - | - | EtOH | Reflux | 120 | - |
| 2 | $ZrFe_2O_4@SiO_2–SO_3H$ | 3 | EtOH | Reflux | 35 | 94 |
| 3 | $ZrFe_2O_4@SiO_2–SO_3H$ | 5 | EtOH | Reflux | 25 | 97 |
| 4 | $ZrFe_2O_4@SiO_2–SO_3H$ | 10 | EtOH | Reflux | 25 | 96 |
| 5 | $ZrFe_2O_4@SiO_2–SO_3H$ | 5 | $H_2O$ | Reflux | 75 | 42 |
| 6 | $ZrFe_2O_4@SiO_2–SO_3H$ | 5 | $H_2O$/EtOH | Reflux | 50 | 72 |
| 7 | $ZrFe_2O_4@SiO_2–SO_3H$ | 5 | EtOH | 100 | 20 | 97 |
| 8 | $ZrFe_2O_4@SiO_2–SO_3H$ | 5 | EtOH | r.t | 90 | 68 |

**Table 2.** Synthesis of Tetrahydrobenzo[b]pyran derivatives

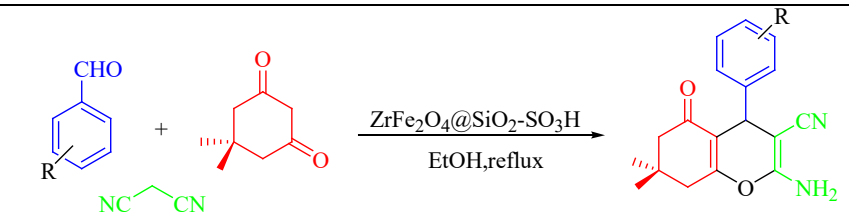


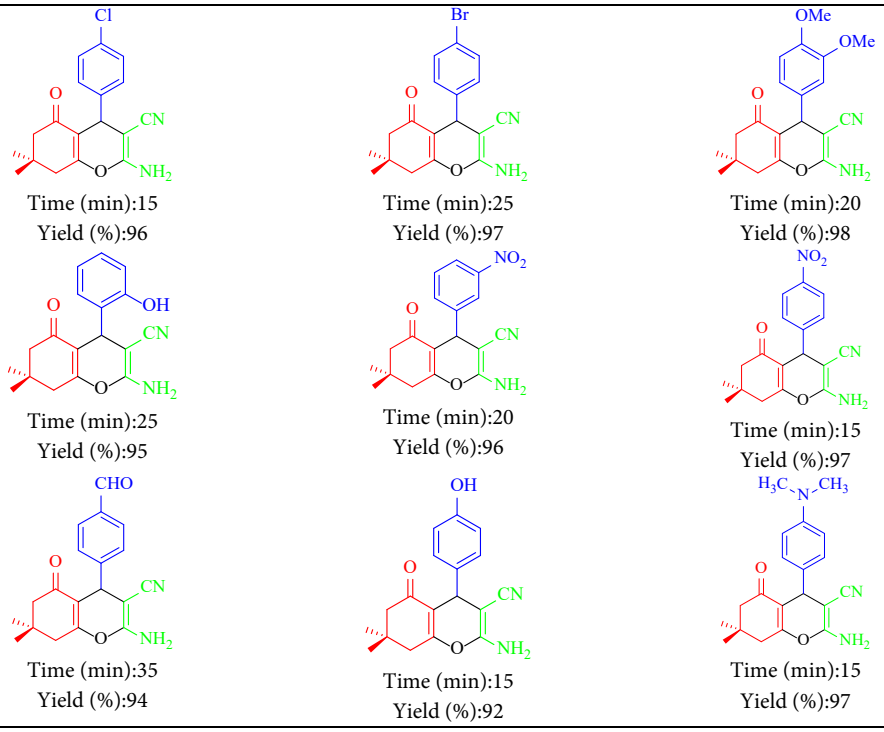


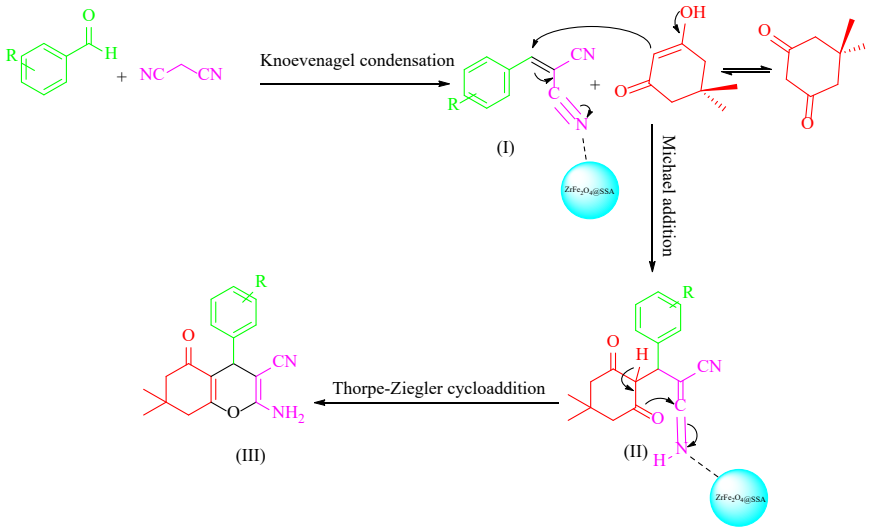


**Scheme 2.** Plausible Mechanism for the Synthesis of Tetrahydrobenzo[b]pyran over the Catalysis of $ZrFe_2O_4$@ $SiO_2$–$SO_3H$

**Table 3.** Comparison of the $ZrFe_2O_4@SiO_2–SO_3H$ Catalyst Activity with Other Reported in the Literature for the Synthesis of Tetrahydrobenzo[b]pyran

| Entry | Synthesis | Catalyst | Time (min) | Yield (%) | Reference |
|---|---|---|---|---|---|
| 1 | Tetrahydrobenzo[b]pyran | GO-ANSA | 30 | 95 | [34] |
| 2 | Tetrahydrobenzo[b]pyran | SAPES@BNPs | 60 | 97 | [35] |
| 3 | Tetrahydrobenzo[b]pyran | $CeO_2/CoFe_2O_4$ | 180 | 90 | [36] |
| 4 | Tetrahydrobenzo[b]pyran | Hal-Py-IL | 90 | 100 | [37] |
| 5 | Tetrahydrobenzo[b]pyran | Cu(II)-Schiff-base$(CH_2)_3@SiO_2@Fe_3O_4$ | 40 | 94 | [38] |
| 6 | Tetrahydrobenzo[b]pyran | $ZrFe_2O_4@SiO_2–SO_3H$ | 25 | 97 | This work |

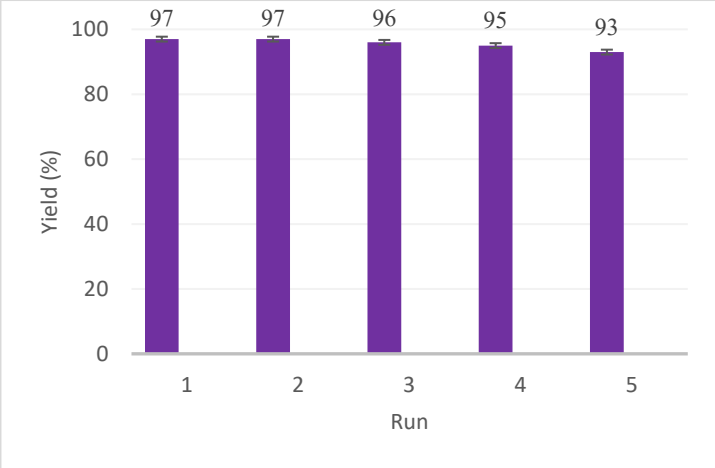


**Fig. 7.** Recycling of the catalyst for the model reaction

important in terms of environmental sustainability and economic efficiency. Therefore, in order to investigate the stability and reusability of the $ZrFe_2O_4@SiO_2–SO_3H$ catalyst, after the completion of the reaction, the catalyst was separated from the reaction using a strong external magnet and used for five consecutive cycles (Figure 7). The results confirmed its stability well, considering the lack of significant decrease in catalyst activity at the end of these cycles.

### *3.4. Comparison*

A comparison between the studied method and the catalysts reported in previous papers was made to further investigate its efficiency. As the results are shown in Table 3, despite the significant advantages in each reported method, the results obtained with the current catalyst showed the reaction to be carried out in a short time with high efficiency, energy saving, and also catalytic properties with recyclability.

## 4. Conclusions

In summary, in this study, magnetic zirconium ferrite nanoparticles were used to stabilize silica sulfonic acid and their efficiency in the synthesis of Tetrahydrobenzo[b]pyran heterocyclic compounds was investigated. The remarkable properties of the two-component combination of black magnetic nanoparticles $ZrFe_2O_4$ with chlorosulfonic acid resulted in the synthesis of a catalyst with remarkable catalytic activity, easy separation and therefore reusability, as well as high stability. Using FT-IR analysis of the mixture, the presence of acidic peaks in the structure was identified. In addition, the spherical morphology of the synthesized nanoparticles as the central core of the catalyst was confirmed using SEM images. One of the most fundamental advantages of the $ZrFe_2O_4@SiO_2–SO_3H$ magnetic nanocatalyst is its easy separation using a strong external magnet, which has enabled its recovery for 5 consecutive cycles. In addition, the easy synthesis method using available and

inexpensive materials, the use of a small amount of catalyst to carry out the target reaction, while achieving high efficiency in a short time, are other advantages of this catalyst.

## Acknowledgements

This work was supported by the research facilities of Ilam University, Ilam, Iran.

## Conflicts of interest

The authors declare that they have no known conflicts of interest.

## Data availability statement

The data that support the findings of this study are available in the supporting information of this article.

## References

[1] I. Ahmad, M. Kedhim, Y. Jadeja, G. Sangwan, A. Kashyap, S. Shomurotova, M. Kazemi, R. Javahershenas, A comprehensive review on carbonylation reactions: catalysis by magnetic nanoparticle-supported transition metals. Nanoscale Advances, 7(11) (2025) 3189-3209. DOI: 10.1039/D5NA00040H

[2] A. Ali, T. Shah, R. Ullah, P. Zhou, M. Guo, M. Ovais, Z. Tan, Y. Rui, Review on recent progress in magnetic nanoparticles: Synthesis, characterization, and diverse applications, Frontiers in chemistry, 9 (2021) 629054. https://doi.org/10.3389/fchem.2021.629054

[3] M. Borzooei, M. Norouzi, M. Mohammadi, Nanomagnetic $ZrFe_2O_4$-Decorated porous silica sulfuric acid as an inorganic solid acid catalyst for synthesis of N-Heterocycles, Langmuir 41 (33) (2025) 22419-22432. https://doi.org/10.1021/acs.langmuir.5c02827

[4] B. Changmai, R. Rano, C. Vanlalveni, SL. Rokhum, A novel Citrus sinensis peel ash coated magnetic nanoparticles as an easily recoverable solid catalyst for biodiesel production, Fuel 286 (2021) 119447. https://doi.org/10.1016/j.fuel.2020.119447

[5] MP. Conte, JK. Sahoo, YM. Abul-Haija, KA. Lau, RV. Ulijn, Biocatalytic self-assembly on magnetic nanoparticles. ACS Applied Materials & Interfaces, 10 (3) (2018) 3069-3075. https://doi.org/10.1021/acsami.7b15456

[6] I. Crăciunescu, GM. Ispas, A. Ciorîta, RP. Turcu, Functionalized Magnetic Nanomaterial Based on $SiO_2$/Ca (OH) 2-Coated Clusters Decorated with Silver Nanoparticles for Dental Applications. Crystals, 15(7) (2025) 615. https://doi.org/10.3390/cryst15070615.

[7] H. Khashei Siuki, P. Ghamari Kargar, G. Bagherzade, New Acetamidine Cu (II) Schiff base complex supported on magnetic nanoparticles pectin for the synthesis of triazoles using click chemistry, Scientific reports, 12 (1) (2022) 3771. https://doi.org/10.1038/s41598-022-07674-7

[8] X. Liang, QL. Li, JT. Li, WB. Zhao, DZ. Yang, YL. Yang, ZT. Zhong, A facile colorimetric sensor based on $Fe_3O_4$ magnetic nanoparticles with intrinsic catalytic activity for the rapid and selective detection of ochratoxin A, Food Chemistry, 474 (2025) 143179. https://doi.org/10.1016/j.foodchem.2025.143179

[9] B. Maleki, H. Atharifar, O. Reiser, R. Sabbaghzadeh, Glutathione-coated magnetic nanoparticles for one-pot synthesis of 1, 4-dihydropyridine derivatives, Polycyclic Aromatic Compounds, 41 (4) (2021) 721-34. https://doi.org/10.1080/10406638.2019.1614639

[10] MD. Nguyen, HV. Tran, S. Xu, TR. Lee, $Fe_3O_4$ nanoparticles: structures, synthesis, magnetic properties, surface functionalization, and emerging applications, Applied Sciences, 11(23) (2021) 11301. https://doi.org/10.3390/app112311301

[11] S. Payamifar, M. Abdouss, AP. Marjani, The application of magnetic nanoparticles based β-cyclodextrin as recoverable catalyst in various organic transformations: An overview, Arabian Journal of Chemistry, (2024) 106080. https://doi.org/10.1016/j.arabjc.2024.106080

[12] A. Manafi Khajeh Pasha, M. Raoufi S, Ghobadi, M. Kazemi M, Biologically active tetrazole scaffolds: Catalysis in magnetic nanocomposites, Synthetic Communications, 50(24) (20220) 3685-716. https://doi.org/10.1080/00397911.2020.1811872

[13] A. Mittal, I. Roy, S. Gandhi, Magnetic nanoparticles: An overview for biomedical applications, Magnetochemistry, 8(9) (2022) 107. https://doi.org/10.3390/magnetochemistry8090107

[14] S. Peiman, B. Maleki, $Fe_3O_4$@ $SiO_2$@ NTMPThio-Cu: a sustainable and eco-friendly approach for the synthesis of heterocycle derivatives using a novel dendrimer template nanocatalyst, Scientific Reports, 14 (1) (2024) 17401. https://doi.org/10.1038/s41598-024-68316-8

[15] D. Wang, C. Deraedt, J. Ruiz, D. Astruc, Magnetic and dendritic catalysts, Accounts of chemical research, 48(7) (2015) 1871-80. https://doi.org/10.1021/acs.accounts.5b00039

[16] Y. Yan, S. Liang, X. Wang, M. Zhang, SM. Hao, X. Cui, Z. Li, Z. Lin, Robust wrinkled $MoS_2$/NC bifunctional electrocatalysts interfaced with single Fe atoms for wearable zinc-air batteries, Proceedings of the National Academy of Sciences, 118(40) (2021) e2110036118. https://doi.org/10.1073/pnas.2110036118

[17] M. Amiri, T. Gholami, O. Amiri, A. Pardakhti, M. Ahmadi, A. Akbari, A. Amanatfard, M. Salavati-Niasari, The magnetic inorganic-organic nanocomposite based on $ZnFe_2O_4$-Imatinib-liposome for biomedical applications, in vivo and in vitro study. Journal of Alloys and Compounds, 849 (2020) 156604. https://doi.org/10.1016/j.jallcom.2020.156604

[18] M. Amiri, M. Salavati-Niasari, A. Akbari, T. Gholami, Removal of malachite green (a toxic dye) from water by cobalt ferrite silica magnetic nanocomposite: herbal and green sol-gel autocombustion synthesis, International Journal of Hydrogen Energy, 42(39) (2017) 24846-60. https://doi.org/10.1016/j.ijhydene.2017.08.077

[19] F. Ansari, F. Soofivand, M. Salavati-Niasari, Utilizing maleic acid as a novel fuel for synthesis of $PbFe_{12}O_{19}$ nanoceramics via sol–gel auto-combustion route. Materials Characterization, 103 (2015) 11-7. https://doi.org/10.1016/j.matchar.2015.03.010

[20] M. Baladi, M. Amiri, M. Amirinezhad, WK. Abdulsahib, F. Pishgouii, Z. Golshani, M. Salavati-Niasari, Green synthesis and characterization of terbium orthoferrite nanoparticles decorated with g-$C_3N_4$ for antiproliferative activity against human cancer cell lines (Glioblastoma, and Neuroblastoma), Arabian Journal of Chemistry, 16 (7) (2023) 104841. https://doi.org/10.1016/j.arabjc.2023.104841

[21] Z. Digbari, R. Monsef, M. Salavati-Niasari, FH. Alsultany, $NiCrFeO_4$ nanostructures: Sonochemical synthesis, characterization and promising photocatalytic application for removal of toxic coloring agents under visible light, Results in Engineering, (2025) 105096. https://doi.org/10.1016/j.rineng.2025.105096

[22] S. Mandizadeh, F. Soofivand, M. Salavati-Niasari, S. Bagheri, Auto-combustion preparation and characterization of $BaFe_{12}O_{19}$ nanostructures by using maleic acid as fuel, Journal of Industrial and Engineering Chemistry, 26 (2015) 167-72. http://dx.doi.org/10.1016/j.jiec.2014.10.044

[23] S. Mazaheri, R. Monsef, FH. Alsultany, M. Salavati-Niasari, Enhanced visible-light-driven photocatalytic potential of magnetic $NiMnFeO_4$/g-$C_3N_4$ nanocomposites for degradation of aqueous organic pollutants: Schiff-base ligand-assisted sol–gel auto-combustion synthesis, characterization and mechanism analysis, Applied Water Science, 15(6) (2025) 130. https://doi.org/10.1007/s13201-025-02469-3

[24] MS. Dehaghani, Z. Esfandiari, M. Khodadadi, Application of L-leucine-based natural deep eutectic solvent and ferroferric oxide magnetic nanoparticles modified with silica and zeolitic imidazolate framework-8 ($Fe_3O_4$@ $SiO_2$@ ZIF-8) for extracting organophosphorus pesticides from cucumber, Food Chemistry, 481 (2025) 143939. https://doi.org/10.1016/j.foodchem.2025.143939

[25] A. Khalid, RM. Ahmed, M. Taha, TS. Soliman, $Fe_3O_4$ nanoparticles and $Fe_3O_4$@ $SiO_2$ core-shell: synthesize, structural, morphological, linear, and nonlinear optical properties, Journal of Alloys and Compounds, 947 (2023) 169639. https://doi.org/10.1016/j.jallcom.2023.169639

[26] S. Mourdikoudis, A. Kostopoulou, AP. LaGrow AP, Magnetic nanoparticle composites: synergistic effects and applications, Advanced Science, 8(12) (2021) 2004951. https://doi.org/10.1002/advs.202004951

[27] A. Czempik, F. Grasset, S. Auguste, A. Rousseau, J. Kubacki, T. Sobol, M. Szczepanik, N. Randrianantoandro, A. Bajorek, Unraveling the effect of annealing on the structural and microstructural evolution of $NiFe_2O_4$@ $SiO_2$ core-shell type nanocomposites, Ceramics International, 50(11) (2024) 20473-94. https://doi.org/10.1016/j.ceramint.2024.03.170

[28] LK. Dhugga, N. Kaur, N. Gill, AL. Sharma, DP. Singh, Tailoring the electrical, dielectric and magnetic properties of $SiO_2$ Coated $NiFe_2O_4$ nanoparticles, Ceramics International, (2025). https://doi.org/10.1016/j.ceramint.2025.06.208

[29] Z. Liu, M. Lei, W. Zeng, Y. Li, B. Li, D. Liu, C. Liu, Synthesis of magnetic $Fe_3O_4$@ $SiO_2$-(-$NH_2$/-COOH) nanoparticles and their application for the removal of heavy metals from wastewater, Ceramics International,49(12) (2023) 20470-9. https://doi.org/10.1016/j.ceramint.2023.03.177

[30] M. Mahdi Eshaghi, M. Pourmadadi, A. Rahdar, AM. Díez-Pascual, Novel carboxymethyl cellulose-based hydrogel with core–shell $Fe_3O_4$@ $SiO_2$ nanoparticles for quercetin delivery, Materials, 15(24) (2022) 8711. https://doi.org/10.3390/ma15248711

[31] M. Sajid, S. Shuja, H. Rong, J. Zhang, Size-controlled synthesis of $Fe_3O_4$ and $Fe_3O_4$@ $SiO_2$ nanoparticles and their superparamagnetic properties tailoring, Progress in Natural Science: Materials International, 33(1) (2023) 116-9. https://doi.org/10.1016/j.pnsc.2022.08.003

[32] M. Talaei, SA. Hassanzadeh-Tabrizi, A. Saffar-Teluri, Synthesis of mesoporous $CuFe_2O_4$@ $SiO_2$ core-shell nanocomposite for simultaneous drug release and hyperthermia applications, Ceramics International, 47(21) (2021) 30287-97. https://doi.org/10.1016/j.ceramint.2021.07.209

[33] M. Yaseen, A. Khan, M. Humayun, S. Farooq, N. Shah, S. Bibi, ZA. Khattak, AU. Rehman, S. Ahmad, SM. Ahmad, M. Bououdina, Facile synthesis of $Fe_3O_4$–$SiO_2$ nanocomposites for wastewater treatment, Macromolecular Materials and Engineering, 308(7) (2023) 2200695. https://doi.org/10.1002/mame.202200695

[34] S. Gharghish, MG. Dekamin, SH. Banakar, Functionalized graphene oxide by 4-amino-3-hydroxy-1-naphthalenesulfonic acid as a heterogeneous nanocatalyst for the one-pot synthesis of tetraketone and tetrahydrobenzo [b] pyran derivatives under green conditions, Nanoscale Advances,6(15) (2024) 3911-22. DOI: 10.1039/D4NA00223G

[35] N. Emad-Abbas, J. Naji, P. Moradi, T. Kikhavani, 3-(Sulfamic acid)-propyltriethoxysilane on biochar nanoparticles as a practical, biocompatible, recyclable and chemoselective nanocatalyst in organic reactions, RSC advances, 14(31) (2024) 22147-58. DOI: 10.1039/D4RA02265C

[36] S. Karizi, M. Ferri, Investigating the Performance of Magnetic Nanocatalyst $CeO_2$/$CoFe_2O_4$ in the Preparation of Tetrahydrobenzo [b] pyrans Derivatives, Nanomaterials Chemistry, 2(2) (2024) 79-94. https://doi.org/10.22034/nc.2024.477972.1036

[37] S. Sadjadi, F. Koohestani, N. Abedian-Dehaghani, MM. Heravi, Halloysite nanoclay with high content of sulfonic acid-based ionic liquid: a novel catalyst for the synthesis of tetrahydrobenzo [b] pyrans, Catalysts, 11(10) (2021) 1172. https://doi.org/10.3390/catal11101172

[38] MH. Galehban, B. Zeynizadeh, H. Mousavi, Diverse and efficient catalytic applications of new cockscomb flower-like $Fe_3O_4$@ $SiO_2$@ KCC-1@ MPTMS@ Cu II mesoporous nanocomposite in the environmentally benign reduction and reductive acetylation of nitroarenes and one-pot synthesis of some coumarin compounds, RSC advances, 12(18) (2022) 11164-89. DOI: 10.1039/D1RA08763K